Geophysical Research Letters

RESEARCH LETTER
10.1029/2018GL080613

Deep Transient Slow Slip Detected by Survey GPS in the Region of Atacama, Chile

E. Klein[1,2,3], Z. Duputel[1], D. Zigone[1], C. Vigny[2], J.-P. Boy[1], C. Doubre[1], and G. Meneses[2]

[1]Institut de Physique du Globe de Strasbourg; UMR 7516, Université de Strasbourg/EOST, CNRS, Strasbourg, France, [2]Laboratoire de géologie, Département de Géosciences, ENS, CNRS, UMR 8538, PSL Research University, Paris, France, [3]Now at Institute of Geophysics and Planetary Physics, Scripps Institution of Oceanography, University of California, San Diego, California, USA

Key Points:
- We detected a transient signal that occurred between 2014 and 2016 in Central North Chile using sGPS data
- We rejected any nontectonic source such as instrumental or hydrological processes
- These observations confirmed by cGPS are explained by slow slip events in the transition zone of the megathrust

Supporting Information:
- Supporting Information S1
- Movie S1

Correspondence to:
E. Klein,
klein@geologie.ens.fr

Citation:
Klein, E., Duputel, Z., Zigone, D., Vigny, C., Boy, J.-P., Doubre, C., & Meneses, G. (2018). Deep transient slow slip detected by survey GPS in the region of Atacama, Chile. *Geophysical Research Letters*, *45*. https://doi.org/10.1029/2018GL080613

Received 24 SEP 2018
Accepted 11 NOV 2018
Accepted article online 15 NOV 2018

Abstract We detected a long-term transient deformation signal between 2014 and 2016 in the Atacama region (Chile) using survey Global Positioning System (GPS) observations. Over an ~150 km along-strike region, survey GPS measurements in 2014 and 2016 deviate significantly from the interseismic trend estimated using previous observations. This deviation from steady state deformation is spatially coherent and reveals a horizontal westward diverging motion of several centimeters, along with a significant uplift. It is confirmed by continuous measurements of recently installed GPS stations. We discard instrumental, hydrological, oceanic, or atmospheric loading effects and show that the transient is likely due to deep slow slip in the transition zone of the subduction interface (~40- to 60-km depth). In addition, daily observations recorded by a continuous GPS station operating between 2002 and 2015 highlight similar transient signals in 2005 and 2009, suggesting a recurrent pattern.

Plain Language Summary The dense development of Global Positioning System (GPS) networks along plate boundaries worldwide has allowed us to observe different fault behaviors: long-term deformation over decades to centuries or the motion generated by major earthquakes. We also observe slow slip events, occurring over weeks to months, creating significant motion without generating seismic waves. These events are observed on most subduction zones on Earth, repeating regularly. Usually occuring at depth larger than 40 km, they are often associated with long-lasting low amplitudes seismic vibrations. Although the Chilean subduction zone is one of the most active on Earth, no such slow event has yet been observed. Using survey GPS observations since 2010 in the region of Atacama (Central North Chile), completed by continuous observations, we have detected a transient signal between 2014 and 2016. After investigating all possible sources, we demonstrate that a deep slow slip event is the most likely origin. Despite a quite sparse seismic network in this region, the seismic observations show an unusual long-lasting low amplitudes seismic activity. Going further, the observations recorded by a GPS station operational since 2002 shows similar signals in 2009 and 2005, highlighting a recurrent pattern of slow slip events in the Atacama region.

1. Introduction

Thanks to the development of Global Positioning System (GPS) networks along plate boundaries in the last 25 years, slow slip events (SSEs) have been detected within the brittle-ductile transition region of various subduction zone interfaces: Japan, Cascadia, Mexico, Costa Rica, New Zealand, Alaska, among others (see Beroza & Ide, 2011; Peng & Gomberg, 2010; Schwartz & Rokosky, 2007, for reviews). These SSEs are characterized by slow aseimic fault creep and are often associated with seismicity on the form of nonvolcanic tremor activity (e.g., Miller et al., 2002; Obara, 2002; Payero et al., 2008; Rogers & Dragert, 2003) and low-frequency earthquakes (e.g., Frank et al., 2013; Hirose & Obara, 2005; Shelly et al., 2007). Although SSEs have been extensively studied over the last decade, physical mechanisms controlling slow slip remain quite elusive (Ikari et al., 2013; Leeman et al., 2016; Romanet et al., 2018; Segall et al., 2010). The influence of SSEs on the seismic cycle and their impact in terms of seismic hazard are also not yet fully understood. Slow slip seems to be closely related to earthquakes as several observations suggest that SSEs may have happened just before or after large seismic events (Kato et al., 2012; Radiguet et al., 2016; Ruiz et al., 2014; Wallace et al., 2017; Zigone et al., 2012).

On the other hand, some SSEs occur quasiperiodically independently of large earthquakes (Rogers & Dragert, 2003; Wallace et al., 2016). Although the Chilean megathrust is one of the most active, with three megathrust earthquakes of $M_w \geq 8$ over the last decade (Illapel 2015, Iquique 2014, Maule 2010, Ruiz et al., 2016, 2014, Vigny et al., 2011), it is one of the only subduction zone where recurrent deep SSEs have not been observed yet. Until recently, the poor coverage of continuous GPS over this 4,000-km-long plate boundary prevented our ability to determine if SSEs occur in the region. In recent years, two aseismic events were observed on the shallow part of the interface (<40 km), both associated with low to moderate seismic activity, and were followed by a significant earthquake: a few weeks to a month-long slip event preceding the 2014 $M_w = 8.1$ Iquique earthquake (Ruiz et al., 2014; Socquet et al., 2017) and a few days-long slip event associated with the 2017 $M_w = 6.9$ Valparaiso earthquake (Ruiz et al., 2017).

Despite the poor continuous GPS instrumentation, decadal-scale interseismic deformation has been intensely monitored thanks to the deployment and yearly measurements of several dense survey GPS (sGPS) networks overlying the plate interface, in the regions of South Central Chile (Moreno et al., 2010; Ruegg et al., 2009), Coquimbo (Khazaradze & Klotz, 2003; Klotz et al., 2001; Métois et al., 2012; Vigny et al., 2009), Atacama (Klein et al., 2018; Métois et al., 2014), and North Chile (Kendrick et al., 2003; Klotz et al., 1999; Métois et al., 2013). The coupling pattern constrained by the resulting interseismic velocity field highlights a heterogeneous segmentation, alternating between coupled segments where megathrust earthquakes are likely to occur and Low Coupling Zones (LCZ), which might act as seismic barriers (Métois et al., 2016).

The region of Atacama (29–25°S) possesses somewhat different characteristics compared to the rest of the subduction zone. Seismic activity on the shallower part of the interface (<30 km) is quite low (Métois et al., 2016) with the exception of the occurrence of regular swarms offshore Caldera (27°S in 1973, 1979, 2006; Holtkamp et al., 2011; Figure 1a). A clear gap in seismicity is also visible at depths greater than 40 km compared to adjacent regions (Figure 1a). Historical seismicity reports two events of $M_w \geq 8.5$ (1819, 1922), both characterized by complex rupture sequences (Willis, 1929). In this region, a sGPS network was installed starting in 2010 and measured yearly to estimate the steady state velocity field and derive the coupling ratio on the megathrust interface (Figure 1a and Figure S1 in the supporting information). The two highly coupled Atacama and Chañaral segments are separated by the Baranquilla LCZ (Klein et al., 2018; Métois et al., 2014), where the aforementioned swarm events occurred (Métois et al., 2016; Figures 1a and 1b; 28°S). However, in a region ~150 km long centered on Copiapó and Caldera (Figure 1), GPS measurements made in 2015 and 2016 deviate from the steady state interseismic trend (Figure 2a). Estimating the static offset from available survey data reveals a spatially coherent pattern of displacements with centimeter-level amplitude. This transient deformation is also consistent with the observations made by the few continuous stations in the area (Figures 1b and 2b), which discard any instrumental errors related to the sGPS processing.

In this study, we investigate the possible origins of this transient signal that can be associated with tectonic or nontectonic sources. In particular, we assess potential effects due to hydrological, oceanic, or atmospheric sources and we investigate if this signal corresponds to episodic aseismic slip.

2. GPS Observations

2.1. Survey GPS Observations

The survey network in Atacama was first installed and measured in 2010, right after the $M_w = 8.8$ Maule earthquake (Métois et al., 2014). Annual surveys have been conducted ever since, jointly with the northward extension of the network in Taltal (Klein et al., 2018). The Central Andes GPS Project (Brooks et al., 2003) and South America Geodynamic Activities (Klotz et al., 2001) GPS marks in the area were remeasured at the same time to gather a data set of almost 70 survey points, measured at least 3 times and up to 7 times (see Table S1 and Klein et al., 2018, for more details about the network and measurements). The sGPS data set is augmented by observations from recently installed cGPS stations operated by the *Centro Sismologico Nacional de Chile* (CSN; Báez et al., 2018), together with a selection of well-distributed permanent stations across the South American continent (International GPS Service; Beutler et al., 1999), (*Red Argentina de Monitoreo Satelital Continuo*; Piñón et al., 2018), and *Rede Brasileira de Monitoramento Contínuo* networks. This data set is processed using a differential approach (GAMIT/GLOBK software), following methods outlined in Herring et al. (2010a, 2010b) and with the same approach used by previous studies in Central North Chile (Klein et al., 2018; Métois et al., 2016; Vigny et al., 2009). Position time series are estimated by combining daily solutions using global sites to define the reference frame in GLOBK because of postseismic deformation following the Maule earthquake which affects many reference stations on the South American continent (Klein et al., 2016).

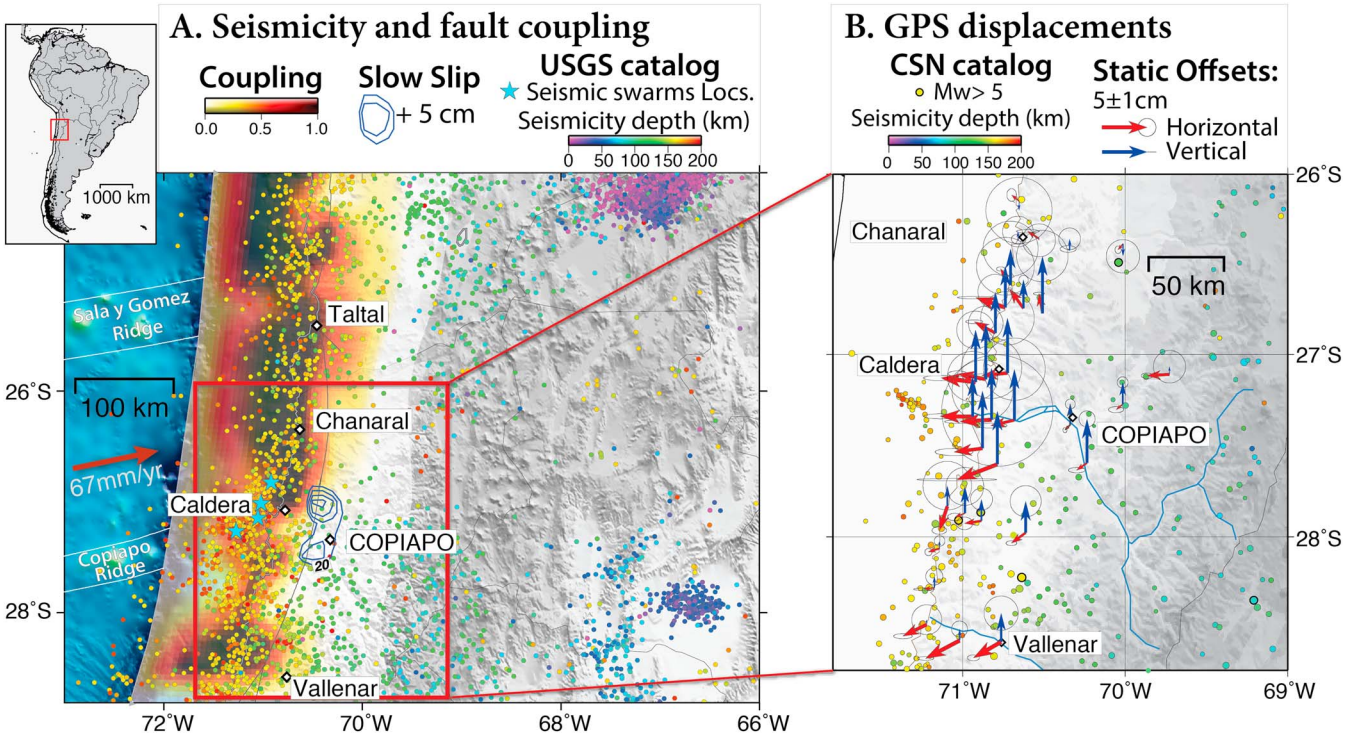

Figure 1. Seismotectonic context. (a) Coupling model and seismicity in the study region. Circles represent earthquake locations from the United States Geological Survey (USGS) catalog (1973–2017) that are colored as function of depth. Blue stars depict locations of seismic swarms in 1973, 1979, 2006, (Holtkamp et al., 2011) and 2015. The red color map shows the coupling model from Klein et al. (2018) obtained using interseismic velocities (see Figure S1). White lines represent main bathymetric features of the Nazca plate (Álvarez et al., 2015). Our preferred SSE slip model is represented with blue contour lines (+5 cm). Inset: Location of the study zone in South America. (b) Static horizontal (red) and vertical (blue) offsets estimated from sGPS time series. Seismicity from the CSN catalog (2014.5–2016) is represented as function of depth (same color scale as in a). SSE = slow slip event; sGPS = survey GPS; CSN = Centro Sismologico Nacional de Chile; GPS = Global Positioning System.

After 7 years of yearly sGPS observations in a very localized area of the Atacama region, the 2016 position deviates significantly from the interseismic trend, both in horizontal and vertical (Figures 2a and S2). While the effect on the horizontal components is significantly smaller, we also observe a similar deviation in the vertical trend in 2015.

We estimate the deviation between the 2016 position predicted by the 2010–2014 trend and the 2016 measured position. The resulting static offsets show a very coherent pattern over an ~150-km region, on both horizontal and vertical components. Horizontal displacement vectors are diverging: northwestward north of Caldera and southwestward south of Caldera (Figure 1b). Vertical offsets are showing a centimeter-level uplift with amplitudes clearly above the noise level, while the interseismic regime is characterized by subsidence (Figure 2a, Up). The northern boundary of this transient signal is marked by a lack of measurable deviation from the 2010–2014 interseismic trend at the latitude of Chañaral (Figure 1b), while the southern one is more difficult to define, due to the coseismic and postseismic deformations associated with the 2015 Illapel earthquake.

Because of such a spatial coherency of the signal, we exclude both instrumental errors during the data acquisition (equipment issues or artificial signal due to the change of equipment; see Table S1) or random errors in the processing parameterization. Furthermore, we rule out any issue in the definition of the reference frame, which would result in a systematic error over the whole area processed and not only in this region.

2.2. Continuous GPS Observations

Until 2015, the Atacama region had poor coverage of cGPS instruments with only one station installed in 2002 in Copiapó (COPO), which was decommissioned in 2015. A few months before COPO was decommissioned, two new nearby stations (BN03 and UDAT) were installed by the CSN. Two other stations were installed at the same period, TAM3 located about 25 km southeast of COPO and LLCH 120 km southwest of COPO (Figure 2c).

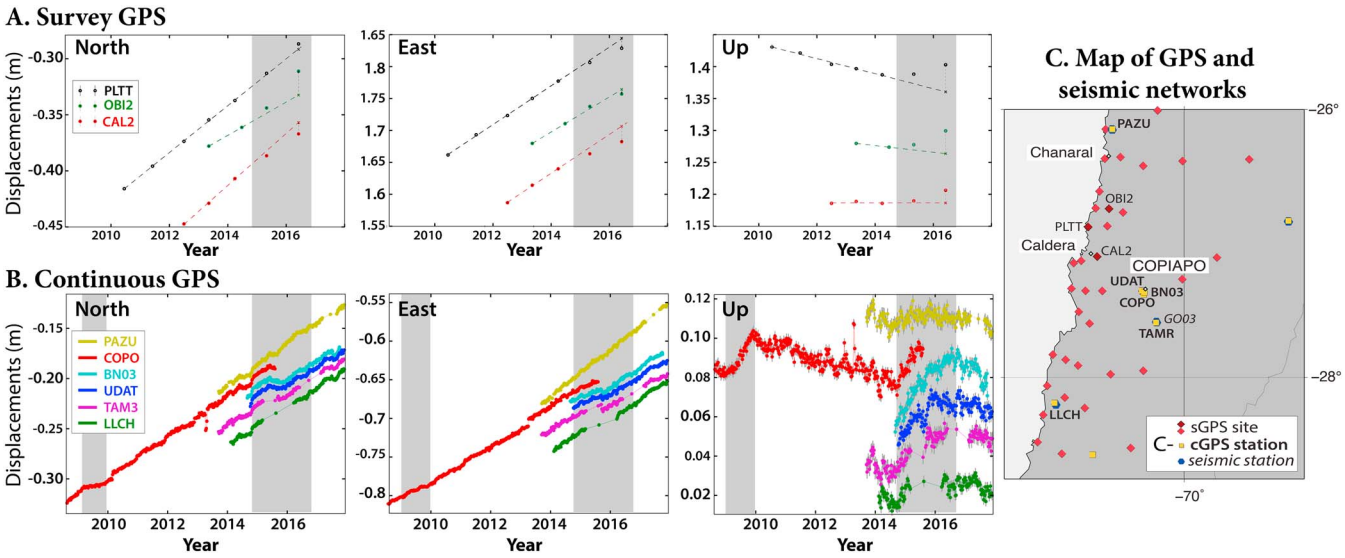

Figure 2. Survey and continuous GPS time series. (a) sGPS annual time series and (b) cGPS weekly time series (downsampled from University of Nevada, Reno (UNR) daily time series). Time series are ordered by latitude of sites and are represented in ITRF08 (Altamimi et al., 2012). Duration of the 2010 and 2014 transients is depicted by gray areas. (c) Location of GPS sites and seismic stations. Detrended time series are presented in Figure S2 of the supporting information. GPS = Global Positioning System.

To confirm that the signal extracted from survey mode data does not artificially result from our differential processing, we investigate the time series of CSN cGPS stations provided by the Nevada Geodetic Laboratory, University of Nevada, Reno (UNR), (Figure 2b) and processed following a different processing strategy (PPP, for more details see http://geodesy.unr.edu/gps/ngl.acn.txt).

All the stations in the region of Copiapó show a clear transient signal starting in mid-2014 that is visible on vertical and horizontal components (Figures 3a and S3). The cGPS station LLCH located south of the region also shows such a signal but with a smaller amplitude, in agreement with the amplitude decrease observed by nearby campaign measurements. Similar to sGPS observations at the latitude of Chañaral (26.4°S), no clear transient displacement is detected on the time series of the station PAZU located 140 km north of Copiapó (Figure 2b). Most of stations shown in Figure 2b have been installed shortly before (PAZU, TAM3, and LLCH) or during (BN03 and UDAT) the transient signal, while COPO was decommissioned before the conclusion of the event. To avoid any inconsistent amplitudes due to such temporal incoherences, we do not estimate any static offset from the cGPS observations. Although sGPS offsets are probably underestimated because they were measured before the end of the transient, they span a common time period and can therefore be used together to constrain a slip model representing that time period. Figure S4 shows that sGPS and cGPS solutions are consistent, which confirms the existence of a transient signal. In the time series of COPO which started in 2002, we observe a similar transient signal in 2009 with a shorter duration but comparable amplitude (Figure 3). We also observe a transient uplift in 2004/2005 with comparable amplitude, although the time series at that time is much noisier. It is difficult to estimate the exact duration of this transient, in the absence of data from the earlier period. Deviations in the horizontal components are also visible during the same time period (Figure S3). Unfortunately, COPO was the only permanent station in operation in the region until 2015 and the survey network was installed starting in 2010.

3. Assessment of Hydrological, Oceanic, and Atmospheric Loading Effects

In 2015, a very strong El Niño event was responsible for large rainfalls in Central North Chile. Smaller rainfalls occurred in May 2010 (probably also related to the strong El Niño event that year) and May 2014 (Figure 3b). Such events could generate variations of hydrostatic pore pressure in underlying aquifer, which could be measurable by GPS (e.g., Silverii et al., 2016). To assess if such effects could explain the observed transient, we gathered rainfall data set in Atacama, in particular at meteorological stations in the city of Copiapó (between 2002 and 2014 from Valdés-Pineda et al., 2018, and from global weather website between 2009 and present day). Significant rainfalls have occurred several months before and after the beginning of the transient (in 2014

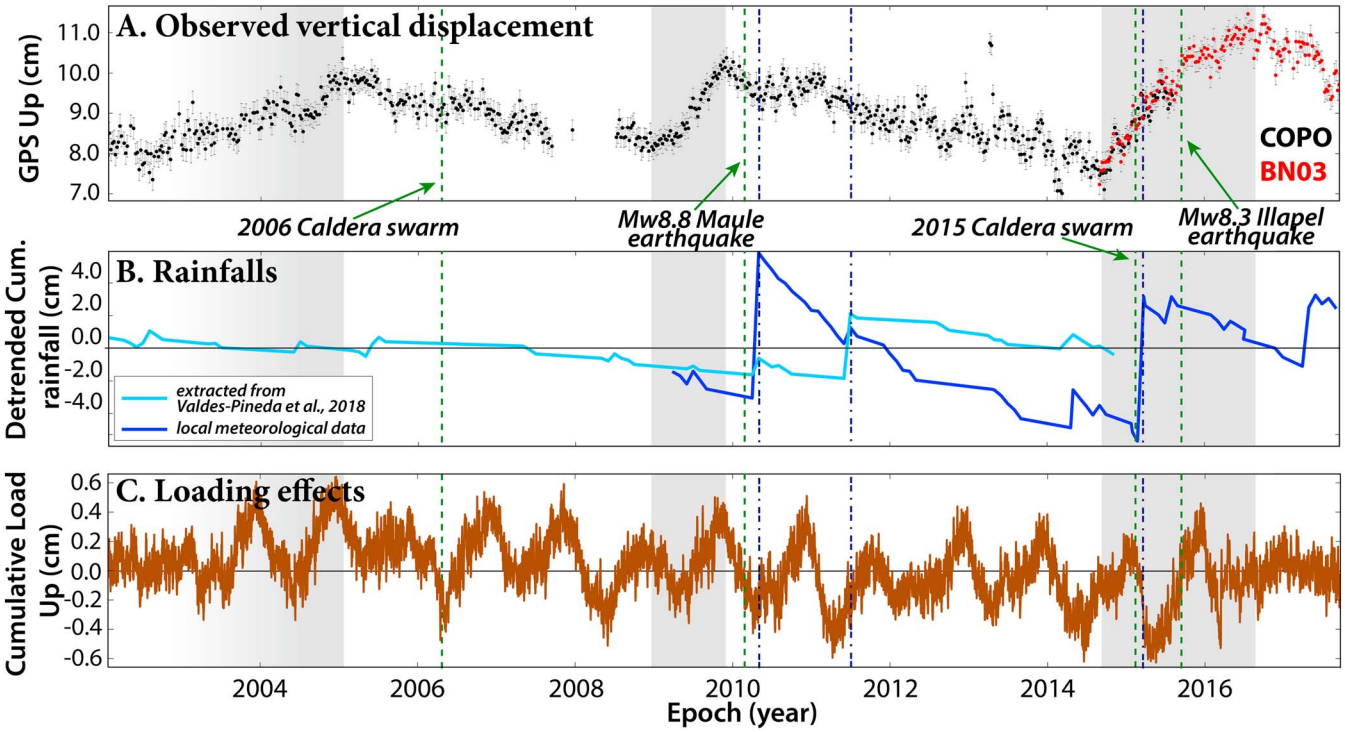

Figure 3. Comparison between observed vertical displacements, rainfalls, and displacements caused by hydrological, oceanic, and atmospheric loads. (a) Weekly vertical time series of COPO (black) and BN03 (red) represented in ITRF08. (b) Detrended cumulative rainfall time series (between 2002 and 2014 from Valdés-Pineda et al., 2018, local meteorological data between 2009 and present day). (c) Cumulative loads (Estimating the Circulation and Climate of the Ocean, European Centre for Medium Range Forecasts Re-Analysis Interim, and GRACE Mascons products) at COPO station. Green dashed lines correspond to the 2006 and 2015 swarms in Caldera, the 2010 M_w8.8 Maule, and 2015 M_w8.3 Illapel earthquakes, blue dashed lines to dates of major rainfalls. Duration of visible transient events is indicated by gray areas. COPO = Copiapó; GPS = Global Positioning System; GRACE = Gravity Recovery And Climate Experiment.

and 2015), but no clear temporal correlation is visible (Figures 3a and 3b). Moreover, any hydrological load should produce subsidence (e.g., Borsa et al., 2014; Wahr et al., 2013) while uplift is observed in 2014–2016.

Going further, we calculate the elastic response due to nontidal oceanic, atmospheric, and hydrological loading effects at our GPS sites (see, e.g., Petrov & Boy, 2004, for more details). Loading predictions are computed, respectively, using the Estimating the Circulation and Climate of the Ocean modeled ocean bottom pressure (ECCO, run kf080h; Wunsch et al., 2009), European Centre for Medium Range Forecasts Weather Re-Analysis Interim surface pressure (ECMWF ERA-interim; Dee et al., 2011), and Global Land Data Assimilation System/Noah v1 snow, soil moisture, and canopy water (GLDAS/Noah v1, Rodell et al., 2004). We also derive surface displacements due to hydrological loading from the National Aeronautics and Space Administration/Goddard Space Flight Center 1° iterated global mascons (NASA/GSFC, updates from Luthcke et al., 2013). Cumulative vertical displacements due to environmental loading contributions predict a vertical signal of less than 1 cm, without any marked transient signal in 2005, 2009, and 2015 (Figures 3c and S5 for the different contributions on the three components). We are therefore confident that the signal measured by GPS is not due to any nontectonic sources such as atmospheric, oceanic, or hydrological loads.

4. Evaluation of Seismotectonic Source

4.1. Postseismic Deformation Following the 2015 M_w = 8.3 Illapel Earthquake

Megathrust earthquakes often trigger continental scale postseismic deformation (e.g., following the 2011 Tohoku earthquake or the 2010 M_w = 8.8 Maule earthquake; Klein et al., 2016; Sun et al., 2015; Trubienko et al., 2014). As the Atacama region is located only ~500 km north of the rupture zone of the 2015 Illapel earthquake (Klein et al., 2017; Ruiz et al., 2016), postseismic deformation following this event could potentially affect the area where we detect the transient. Nevertheless, this M_w = 8.3 earthquake was significantly smaller than the Maule earthquake, consequently triggering significantly smaller postseismic deformation. In addition, postseismic deformation at such distances from the rupture zone is most likely due to viscoelastic relaxation in the asthenosphere, therefore generating a very long wavelength horizontal surface

motion pointing toward the coseismic rupture zone, that is, southwestward (Klein et al., 2016). The short-scale divergent pattern shown in Figure 1b at the latitude of Copiapó (27.5°S) is thus not consistent with such broad-scale postseismic deformation. However, the southward horizontal motion observed around Vallenar (28°S) could possibly correspond to the postseismic signal of the 2015 Illapel earthquake. These two regions are separated by smaller displacements around 28.2°S, which clearly delineates two zones affected by distinct deformation sources.

4.2. Aseismic Slip on the Interface

After ruling out any strong postseismic signal in the region, an obvious tectonic source able to generate such a spatially coherent transient deformation is aseismic slip along the subduction interface. As presented in section 1, this area is characterized by relatively little seismic activity at depth larger than 40 km (Figure 1a). In addition, no significant earthquake in the Atacama region, able to induce such a deformation, occurred when the 2014 transient started. In the following, we use a Bayesian approach to explore how such slip at the interface can explain our observations.

4.2.1. Bayesian Modeling Strategy

We build a fault geometry with triangular patches based on the finite element mesh designed in Klein et al. (2016, 2017) from Slab1.0 (Hayes et al., 2012) between 28° and 26°S down to 70-km depth.

The forward problem is defined as $\mathbf{d} = \mathbf{Gm}$ with $\mathbf{d}$, the vector containing GPS offsets, and $\mathbf{m}$ the slip model parameters. We assume a pure along-dip faulting, and Green functions $\mathbf{G}$ are calculated at each node of the fault plane, assuming a homogeneous elastic half-space (Okada, 1985). The model space is explored using AlTar, a parallel Monte Carlo approach (Duputel et al., 2015; Jolivet et al., 2015; Minson et al., 2013) to derive the posterior probability density function (PDF) of the model $\mathbf{m}$ given available observations $\mathbf{d}_{\text{obs}}$

$$p(\mathbf{m}|\mathbf{d}_{\text{obs}}) \propto p(\mathbf{m}) \exp\left(-\frac{1}{2}(\mathbf{d}_{\text{obs}} - \mathbf{Gm})^T \mathbf{C}_d^{-1} (\mathbf{d}_{\text{obs}} - \mathbf{Gm})\right) \quad (1)$$

$\mathbf{C}_d$ is the covariance matrix describing observational uncertainties. $p(\mathbf{m})$ is the prior PDF, defined as centered truncated Gaussian with a standard deviation of 25 cm bounded between −1 cm (small back slip is allowed to ensure correct sampling near zero) and 50 cm (Figure S6).

4.2.2. Results

Given large uncertainties (±2 cm) on vertical displacements, we first develop a solution based only on horizontal components. The resulting posterior mean slip distribution is presented in (Figure 4a). This distribution depicts significant slip between 40- and 60-km depth with a peak slip larger than 50 cm. This deep slip patch is associated with a geodetic moment of $2.93 \cdot 10^{19}$ N.m ($M_w = 6.9$; see M_w PDF in Figure 4 and Text S1). As shown in Figure 4c, this solution reproduces the observed horizontal displacements and also the vertical ones not included in the inversion. Because displacements extracted from sGPS observations are associated with significant uncertainties (about 1 cm in horizontal, Figure 1b), there are significant posterior uncertainties on the slip distribution, of the order of 10 cm (Figure 4b and blue slip PDFs in Figure 4a). Both the posterior mode model (representing the maximum of each parameter marginal PDF) and the median model are presented in Figure S7 together with Movie S1 showing more than a thousand model realizations from the space of possible solutions. The variability of the slip at shallow depths reflects high uncertainties in this part of the model. Nonetheless, the deep patch of slip remains quite stable, especially at 27°S on almost every model.

We also conducted an inversion using both horizontal and vertical observations. The posterior mean slip distribution shown in Figure S8 presents a slightly smaller slip amplitude with an equivalent geodetic moment of $2.72 \cdot 10^{19}$ N.m. In particular, approximately 15 cm of slip is needed to fit the data in the southern part of the fault (27.5°S), while more than 25 cm is required for the horizontal displacement based model. Nevertheless, the overall slip distribution is consistent for both models, with similar amplitudes in the main slip area (PDFs in Figure 4a). As expected, integrating more observations results in slightly smaller posterior slip uncertainties on the deep patch (Figure 4a, red PDFs, and Figure S8). Finally, we tested a model with broader priors, producing similar spatial slip distribution, M_w, and data fit (Figure S9). Therefore, we are confident that the overall pattern of slow slip distribution is fairly well defined.

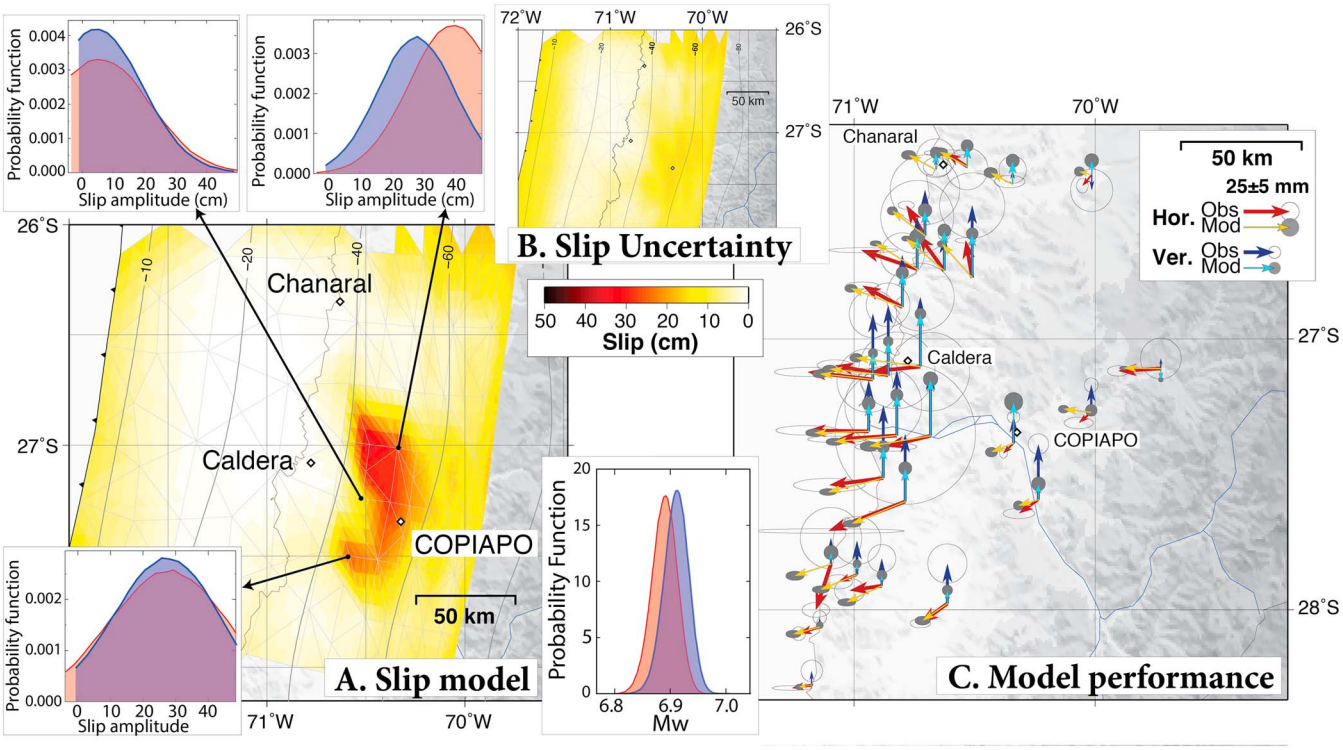

Figure 4. Bayesian modeling of deep aseismic slip. (a) Mean posterior slip distribution (color scale in centimeters). Insets show posterior marginal probability density functions (in blue) at three different locations of the subduction interface, indicated by arrows. Red probability density functions depict the model inverted with both horizontal and vertical components (cf., Figure S8b) 1σ posterior slip uncertainties represented with the same color scale as the slip distribution. (c) Predicted horizontal (yellow) and vertical (light blue) offsets and their associated 2σ uncertainties (filled gray ellipses) compared to measured horizontal (dark red) and vertical (dark blue) displacements.

5. Discussion and Conclusions

In this study, we report observations of a transient deformation signal, initially detected by the sGPS network, on the Atacama region along the Chilean subduction zone. We interpret this signal as a deep aseismic slip event on the subduction interface.

We carefully verified that observed GPS deviations cannot be explained by any nontectonic sources. Because the transient is revealed by both sGPS and cGPS observations which were processed independently, any instrumental errors are very unlikely. We also eliminated any oceanic, hydrological, or atmospheric sources. Although sGPS alone does not allow to accurately constrain the temporal evolution of this event, the compilation of cGPS time series in the region shows that this event started in September 2014 and lasted until mid-2016 (i.e., duration longer than 1 year).

Using a Bayesian modeling approach, we demonstrate that deep slow slip along the subduction interface can explain the observed GPS deviations. The event released a scalar moment equivalent to a $M_w = 6.9$, and its long duration (more than a year) is consistent with the duration versus magnitude scaling laws for slow earthquakes proposed by Ide et al. (2007). The inversion places the SSE downdip of the seismogenic zone (between 40- and 60-km depths; Figure 1a) in the so-called transition zone, which is commonly observed for SSEs in others subduction zones (Obara & Kato, 2016; Rolandone et al., 2018; Schwartz & Rokosky, 2007). This deep SSE in Atacama differs from the recently reported aseismic events in Chile on the shallower part of the interface preceding the occurrence of large earthquakes (Ruiz et al., 2017; Socquet et al., 2017).

Because of the sparse regional seismic network, it is difficult to discern nonvolcanic tremor activity, which is commonly observed in many subduction zones during SSEs (e.g., Cascadia, Mexico, and Japan; Obara, 2002; 2011; Payero et al., 2008; Rogers & Dragert, 2003; Zigone et al., 2012). Only one seismological station is available in the vicinity of the 2014–2016 SSE (GO03; Figure 2c). Some bursts of energy of a few decibels above the average could indicate tremor activities (for more details about the methodology, see Text S3; Husker et al., 2010; Kostoglodov et al., 2010; and Figure S10), but it is unclear whether such signal is tectonic or is associated

with random fluctuations of high-frequency noise. Additional seismic stations in the region would be necessary to further investigate the occurrence of the nonvolcanic tremor and its relationship with the deep slow slip deduced from GPS data.

Another interesting aspect is the possible interaction between SSE and repeated occurrences of seismic swarms offshore Caldera over the last 50 years (in 1973, 1979, and 2006; Holtkamp et al., 2011; and in 2015, CSN catalog, Figure 1b). Seismic swarms are often accompanied by significant magnitude earthquakes ($M_w \geq 6.5$ in 2006; Ducret, 2013; Figure S3) and can be markers of aseismic slip on the interface (e.g., Ruiz et al., 2017). Our tests (presented in Text S2 and Figure S11) show that the observed GPS transient is most likely not associated with seismic or aseismic slip in the area of the March 2015 swarm that occurred at shallow depth (~20 km). In particular, shallow slip on the interface produces subsidence inland rather than uplift. Nonetheless, an indirect link between the deep transient event and the seismic swarms offshore Caldera should be more thoroughly investigated in the future.

Two additional transient signals observed on the COPO time series (Figure 3) suggest that similar SSEs might have occurred in 2005 and 2009. Based on this single cGPS station, the 2009 event seems to last for about 12 months, while the 2005 event is probably shorter (although it is hard to precisely define its beginning). Such recurrence is similar to long-term SSEs reported in southwest Japan, New Zealand, and Mexico (Hirose & Obara, 2005; Radiguet et al., 2012; Wallace & Beavan, 2010), which typically occur every 3–4 years with a scalar moment equivalent to a $M_w = 7$.

To our knowledge, this is the first observation of potentially recurrent deep SSEs reported in Chile. It raises key questions regarding the stress release mechanism along this segment of the Chilean subduction zone and potential interactions between slow slip asperities in the transition zone and megathrust asperities at seismogenic depths.

The shallower part of the interface is characterized by high coupling down to 40 km on the Atacama and Chañaral segments. These two segments are separated by a low coupled portion, the Baranquilla LCZ, which is located at the same latitude as the SSE reported in this study (27°S; Klein et al., 2018; Métois et al., 2013). Note that 2016 measurements have been excluded from the later interseismic model in order to capture the coupling of the subduction interface between SSEs. The modeled slow slip therefore lies below the coupled seismogenic zone with two main slip asperities that seems to be separated by a narrow creeping area (Figure 1a). The comparison of mean slip deficit in the SSE area with the slip inferred from this study is not entirely conclusive. The coupling ratio appears too low at these depths to accumulate in 4 years the 15 cm of slip released by the 2015 SSE (i.e., assuming that the 2009 SSE released all of the previously accumulated stress). However, both the coupling and the slow slip models are associated with significant uncertainties at such depths and the PDF of both models show a significant overlap (Figure S12). While we cannot completely rule out a small contamination of Klein et al.'s (2018) coupling model by measurements at the onset of the SSE in 2015, the above conclusion seems also consistent with the coupling values reported in models constrained before 2014 (Métois et al., 2013, 2016). Although it is difficult to conclude from a single GPS station, the difference in duration between the 2009 and 2014 transients could suggest that both events are different and therefore possibly not perfectly colocated. It could also suggest that the 2009 event did not release all of the previously accumulated stress where the 2015 SSE occurred. In any case, the interplay between interface locking and SSE in this region needs further investigation based on future observations.

The occurrence of deep SSEs also has impact in terms of seismic hazard. In particular, aseismic slip in the transition zone can potentially trigger earthquakes in the seismogenic zone. A similar mechanism has recently been proposed in Mexico where the 2014 SSE is believed to have triggered the $M_w = 7.3$ Papanoa earthquake by either increasing the static stress in the coupled region or by helping the weakening of the earthquake hypocentral area (Radiguet et al., 2016). The occurrence of transient aseismic slip in Chile can thus potentially influence the seismic cycle by changing the stress level in the seismogenic zone, which may advance or delay the occurrence of the next earthquake in the region.

Given the limited amount of observations available until recently, it is obvious that denser deployments of geodetic and seismic instruments are necessary to better capture the behavior of the megathrust in the Atacama region. The launch of new Synthetic Aperture Radar satellite constellations such as the Sentinel-1 mission can also help to monitor and detect transient deformations in sparsely instrumented regions (e.g., Rousset et al., 2016). Such improvements of our observational capabilities also open up new opportunities to

investigate the potential impact of deep SSEs on the shallower part of the interface in Atacama where the last major event occurred almost a century ago.

Acknowledgments
This work was performed in the frame of the French-Chilean LiA *Montessus de Ballore* with financial support of Agence Nationale de la Recherche (projects ANR-2012-BS06-004 and ANR-17-ERC3-0010), the European Research Council (ERC) under the European Union's Horizon 2020 research and innovation programme (grant agreement: 805256), and the Marie Curie Initial Training Network *Zooming in between plates* (ITN FP7 grant agreement 604713). We are also thankful to the Institut National des Sciences de l'Univers (INSU-CNRS) and the Réseau Sismologique & Géodésique Français (RESIF, as part of the *Investissements d'Avenir* program, ANR-11-EQPX-0040, and the French Ministry of Ecology, Sustainable Development and Energy) for providing the geodetic instruments for all campaigns. We would like to warmly thank all CSN staff, for their precious help for the fieldwork. We thank Mark Simons (CalTech) for providing the AITar code used in this study. The authors would also like to sincerely thank Sergio Ruiz (University of Chile), Francesca Silverii, Adrian Borsa (IGPP, SIO), Romain Jolivet, and Sabrina Speich (ENS, Paris) for fruitful discussions. We would like to thank the reviewers for thorough reviews of this manuscript. We are particularly grateful to Laura Wallace for her very thorough and constructive comments that helped us to really improve this study. We also sincerely thank Dara Goldberg who helped us improve the English language usage of the manuscript. All the figures have been made using Generic Mapping Tools GMT (Wessel et al., 2013) using topography from ETOPO5. Data availability: Solutions of continuous GPS data collected by CSN cGPS stations are available through the UNR website (http://geodesy.unr.edu/ http://geodesy.unr.edu/). Interseismic survey measurements used here have been published previously (Klein et al., 2018), and additional measurements are available upon request. Seismic data collected are available through the Incorporated Research Institutions for Seismology (IRIS) Data Management Center.

References

Altamimi, Z., Métivier, L., & Collilieux, X. (2012). ITRF2008 plate motion model. *Journal of Geophysical Research*, *117*, B07402. https://doi.org/10.1029/2011JB008930

Álvarez, O., Gimenez, M., Folguera, A., Spagnotto, S., Bustos, E., Baez, W., & Braitenberg, C. (2015). New evidence about the subduction of the Copiapó ridge beneath South America, and its connection with the Chilean-Pampean flat slab, tracked by satellite GOCE and EGM2008 models. *Journal of Geodynamics*, *91*, 65–88.

Báez, J., Leyton, F., Troncoso, C., del Campo, F., Bevis, M., Vigny, C., et al. (2018). *The Chilean GNSS network: Current status and progress toward early warning applications*, vol. 89, pp. 1546–1554.

Beroza, G. C., & Ide, S. (2011). Slow earthquakes and nonvolcanic tremor. *Annual Review of Earth and Planetary Sciences*, *39*, 271–296.

Beutler, G., Rothacher, M., Schaer, S., Springer, T., Kouba, J., & Neilan, R. (1999). The International GPS Service (IGS): An interdisciplinary service in support of Earth sciences. *Advances in Space Research*, *23*(4), 631–653.

Borsa, A. A., Agnew, D. C., & Cayan, D. R. (2014). Ongoing drought-induced uplift in the western United States. *Science*, *345*(6204), 1587–1590.

Brooks, B. A., Bevis, M., Smalley, R., Kendrick, E., Manceda, R., Lauría, E., et al. (2003). Crustal motion in the southern Andes (26° –36°S): Do the Andes behave like a microplate? *Geochemistry, Geophysics, Geosystems*, *4*(10), 1085. https://doi.org/10.1029/2003GC000505

Dee, D. P., Uppala, S., Simmons, A., Berrisford, P., Poli, P., Kobayashi, S., et al. (2011). The ERA-Interim reanalysis: Configuration and performance of the data assimilation system. *Quarterly Journal of the Royal Meteorological Society*, *137*(656), 553–597.

Ducret, G. (2013). Mesure De Déformation Par Interférométrie Radar: Développements Méthodologiques Et Applications à La Subduction Chilienne (Ph.D Thesis), Laboratoire de Géologie, Ecole Normale Supérieure de Paris.

Duputel, Z., Jiang, J., Jolivet, R., Simons, M., Rivera, L., Ampuero, J.-P., et al. (2015). The Iquique earthquake sequence of April 2014: Bayesian modeling accounting for prediction uncertainty. *Geophysical Research Letters*, *42*, 7949–7957. https://doi.org/10.1002/2015GL065402

Frank, W. B., Shapiro, N. M., Kostoglodov, V., Husker, A. L., Campillo, M., Payero, J. S., & Prieto, G. A. (2013). Low-frequency earthquakes in the Mexican Sweet Spot. *Geophysical Research Letters*, *40*, 2661–2666. https://doi.org/10.1002/grl.50561

Hayes, G. P., Wald, D. J., & Johnson, R. L. (2012). Slab1. 0: A three-dimensional model of global subduction zone geometries. *Journal of Geophysical Research*, *117*, B01302. https://doi.org/10.1029/2011JB008524

Herring, T., King, R., & McClusky, S. C. (2010a). GAMIT : GPS Analysis at MIT, release 10.4.

Herring, T., King, R., & McClusky, S. C. (2010b). GLOBK : Global Kalman filter VLBI and GPS analysis program release 10.4.

Hirose, H., & Obara, K. (2005). Repeating short-and long-term slow slip events with deep tremor activity around the Bungo channel region, southwest Japan. *Earth, planets and space*, *57*(10), 961–972.

Holtkamp, S. G., Pritchard, M. E., & Lohman, R. B. (2011). Earthquake swarms in South America. *Geophysical Journal International*, *187*(1), 128–146. https://doi.org/10.1111/j.1365-246$\times$.2011.05137.x

Husker, A., Peyrat, S., Shapiro, N., & Kostoglodov, V. (2010). Automatic non-volcanic tremor detection in the mexican subduction zone. *Geofi,sica Internacional*, *49*(1), 17–25.

Ide, S., Beroza, G. C., Shelly, D. R., & Uchide, T. (2007). A scaling law for slow earthquakes. *Nature*, *447*(7140), 76–79.

Ikari, M. J., Marone, C., Saffer, D. M., & Kopf, A. J. (2013). Slip weakening as a mechanism for slow earthquakes. *Nature Geoscience*, *6*(6), 468–472.

Jolivet, R., Simons, M., Agram, P., Duputel, Z., & Shen, Z.-K. (2015). Aseismic slip and seismogenic coupling along the central San Andreas Fault. *Geophysical Research Letters*, *42*, 297–306. https://doi.org/10.1002/2014GL062222

Kato, A., Obara, K., Igarashi, T., Tsuruoka, H., Nakagawa, S., & Hirata, N. (2012). Propagation of slow slip leading up to the 2011 Mw 9.0 Tohoku-Oki earthquake. *Science*, *335*(6069), 705–708.

Kendrick, E., Bevis, M., Smalley, R., Brooks, B., Vargas, R. B., Laurıa, E., & Fortes, L. P. S. (2003). The Nazca–South America Euler vector and its rate of change. *Journal of South American Earth Sciences*, *16*(2), 125–131.

Khazaradze, G., & Klotz, J. (2003). Short-and long-term effects of GPS measured crustal deformation rates along the south central Andes. *Journal of Geophysical Research*, *108*(B6), 2289. https://doi.org/10.1029/2002JB001879

Klein, E., Fleitout, L., Vigny, C., & Garaud, J. (2016). Afterslip and viscoelastic relaxation model inferred from the large scale postseismic deformation following the 2010 Mw 8.8 Maule earthquake (Chile). *Geophysical Journal International*, *205*(3), 1455–1472. https://doi.org/10.1093/gji/ggw086

Klein, E., Métois, M., Meneses, G., Vigny, C., & Delorme, A. (2018). Bridging the gap between North and Central Chile: Insight from new GPS data on coupling complexities and the Andean sliver motion. *Geophysical Journal International*, *213*(3), 1924–1933.

Klein, E., Vigny, C., Fleitout, L., Grandin, R., Jolivet, R., Rivera, E., & Métois, M. (2017). A comprehensive analysis of the 2015 Mw 8.3 Illapel earthquake from GPS and inSAR data. *Physics of the Earth and Planetary Interiors*, *469*, 123–134.

Klotz, J., Angermann, D., Michel, G., Porth, R., Reigber, C., Reinking, J., et al. (1999). GPS-derived deformation of the Central Andes including the 1995 Antofagasta $M_w = 8.0$ earthquake. *Pure and Applied Geophysics*, *154*, 709–730.

Klotz, J., Khazaradze, G., Angermann, D., Reigber, C., Perdomo, R., & Cifuentes, O. (2001). Earthquake cycle dominates contemporary crustal deformation in central and southern Andes. *Earth and Planetary Science Letters*, *193*(3), 437–446.

Kostoglodov, V., Husker, A., Shapiro, N. M., Payero, J. S., Campillo, M., Cotte, N., & Clayton, R. (2010). The 2006 slow slip event and nonvolcanic tremor in the Mexican subduction zone. *Geophysical Research Letters*, *37*, L24301. https://doi.org/10.1029/2010GL045424

Leeman, J. R., Saffer, D. M., Scuderi, M. M., & Marone, C. (2016). Laboratory observations of slow earthquakes and the spectrum of tectonic fault slip modes. *Nature Communications*, *7*, 11104.

Luthcke, S. B., Sabaka, T., Loomis, B., Arendt, A., McCarthy, J., & Camp, J. (2013). Antarctica, Greenland and Gulf of Alaska land-ice evolution from an iterated GRACE global mascon solution. *Journal of Glaciology*, *59*(216), 613–631.

Métois, M., Socquet, A., Vigny, C., Carrizo, D., Peyrat, S., Delorme, A., et al. (2013). Revisiting the north Chile seismic gap segmentation using GPS-derived interseismic coupling. *Geophysical Journal International*, *194*(3), 1283–1294. https://doi.org/10.1093/gji/ggt183

Métois, M., Vigny, C., & Socquet, A. (2012). Interseismic coupling, segmentation and mechanical behavior of the central Chile subduction zone. *Journal of Geophysical Research*, *117*, B03406. https://doi.org/10.1029/2011JB008736

Métois, M., Vigny, C., & Socquet, A. (2016). Interseismic coupling, megathrust earthquakes and seismic swarms along the Chilean subduction zone (38–18°S). *Pure and Applied Geophysics*, *173*(5), 1431–1449.

Métois, M., Vigny, C., Socquet, A., Delorme, A., Morvan, S., Ortega, I., & Valderas-Bermejo, C.-M. (2014). GPS-Derived interseismic coupling on the subduction and seismic hazards in the Atacama region, Chile. *Geophysical Journal International*, *196*(2), 644–655. https://doi.org/10.1093/gji/ggt418

Miller, M. M., Melbourne, T., Johnson, D. J., & Sumner, W. Q. (2002). Periodic slow earthquakes from the Cascadia subduction zone. *Science*, *295*(5564), 2423–2423.

Minson, S., Simons, M., & Beck, J. (2013). Bayesian inversion for finite fault earthquake source models I—Theory and algorithm. *Geophysical Journal International*, *194*, 1701–1726.

Moreno, M., Rosenau, M., & Oncken, O. (2010). 2010 Maule earthquake slip correlates with pre-seismic locking of Andean subduction zone. *Nature*, *467*(7312), 198–202. https://doi.org/10.1038/nature09349

Obara, K. (2002). Nonvolcanic deep tremor associated with subduction in southwest Japan. *Science*, *296*(5573), 1679–1681.

Obara, K. (2011). Characteristics and interactions between non-volcanic tremor and related slow earthquakes in the Nankai subduction zone, southwest Japan. *Journal of Geodynamics*, *52*(3-4), 229–248.

Obara, K., & Kato, A. (2016). Connecting slow earthquakes to huge earthquakes. *Science*, *353*(6296), 253–257.

Okada, Y. (1985). Surface deformation due to shear and tensile faults in a half-space. *Bulletin of the seismological society of America*, *75*(4), 1135–1154.

Payero, J. S., Kostoglodov, V., Shapiro, N., Mikumo, T., Iglesias, A., Pérez-Campos, X., & Clayton, R. W. (2008). Nonvolcanic tremor observed in the Mexican subduction zone. *Geophysical Research Letters*, *35*, L07305. https://doi.org/10.1029/2007GL032877

Peng, Z., & Gomberg, J. (2010). An integrated perspective of the continuum between earthquakes and slow-slip phenomena. *Nature Geoscience*, *3*(9), 599.

Petrov, L., & Boy, J.-P. (2004). Study of the atmospheric pressure loading signal in very long baseline interferometry observations. *Journal of Geophysical Research*, *109*, B03405. https://doi.org/10.1029/2003JB002500

Piñón, D. A., Gómez, D. D., Smalley, Jr. R., Cimbaro, S. R., Lauría, E. A., & Bevis, M. G. (2018). The history, state, and future of the Argentine continuous satellite monitoring network and its contributions to geodesy in Latin America. *Seismological Research Letters*, *89*(2A), 475–482.

Radiguet, M., Cotton, F., Vergnolle, M., Campillo, M., Walpersdorf, A., Cotte, N., & Kostoglodov, V. (2012). Slow slip events and strain accumulation in the Guerrero gap, Mexico. *Journal of Geophysical Research*, *117*, B04305. https://doi.org/10.1029/2011JB008801

Radiguet, M., Perfettini, H., Cotte, N., Gualandi, A., Valette, B., Kostoglodov, V., et al. (2016). Triggering of the 2014 Mw 7.3 Papanoa earthquake by a slow slip event in Guerrero, Mexico. *Nature Geoscience*, *9*(11), 829.

Rodell, M., Houser, P., Jambor, U., Gottschalck, J., Mitchell, K., Meng, C., et al. (2004). The global land data assimilation system. *Bulletin of the American Meteorological Society*, *85*(3), 381–394.

Rogers, G., & Dragert, H. (2003). Episodic tremor and slip on the Cascadia subduction zone: The chatter of silent slip. *Science*, *300*(5627), 1942–1943.

Rolandone, F., Nocquet, J.-M., Mothes, P. A., Jarrin, P., Vallée, M., Cubas, N., et al. (2018). Areas prone to slow slip events impede earthquake rupture propagation and promote afterslip. *Science Advances*, *4*(1), eaao6596.

Romanet, P., Bhat, H. S., Jolivet, R., & Madariaga, R. (2018). Fast and slow slip events emerge due to fault geometrical complexity. *Geophysical Research Letters*, *45*, 4809–4819. https://doi.org/10.1029/2018GL077579

Rousset, B., Jolivet, R., Simons, M., Lasserre, C., Riel, B., Milillo, P., et al. (2016). An aseismic slip transient on the North Anatolian Fault. *Geophysical Research Letters*, *43*, 3254–3262. https://doi.org/10.1002/2016GL068250

Ruegg, J.-C., Rudloff, A., Vigny, C., Madariaga, R., de Chabalier, J., Campos, J., et al. (2009). Interseismic strain accumulation measured by GPS in the seismic gap between Constitución and Concepción in Chile. *Physics of the Earth and Planetary Interiors*, *175*(1-2), 78–85.

Ruiz, S., Aden-Antoniow, F., Baez, J., Otarola, C., Potin, B., DelCampo, F., et al. (2017). Nucleation phase and dynamic inversion of the Mw 6.9 Valparaíso 2017 earthquake in Central Chile. *Geophysical Research Letters*, *44*, 10,290–10,297. https://doi.org/10.1002/2017GL075675

Ruiz, S., Klein, E., del Campo, F., Rivera, E., Poli, P., Metois, M., et al. (2016). The seismic sequence of the 16 September 2015 M w 8.3 Illapel, Chile, earthquake. *Seismological Research Letters*, *87*(4), 789–799.

Ruiz, S., Metois, M., Fuenzalida, A., Ruiz, J., Leyton, F., Grandin, R., et al. (2014). Intense foreshocks and a slow slip event preceded the 2014 Iquique Mw 8.1 earthquake. *Science*, *345*(6201), 1165–1169.

Schwartz, S. Y., & Rokosky, J. M. (2007). Slow slip events and seismic tremor at circum-Pacific subduction zones. *Reviews of Geophysics*, *45*, RG3004. https://doi.org/10.1029/2006RG000208

Segall, P., Rubin, A. M., Bradley, A. M., & Rice, J. R. (2010). Dilatant strengthening as a mechanism for slow slip events. *Journal of Geophysical Research*, *115*, B12305. https://doi.org/10.1029/2010JB007449

Shelly, D. R., Beroza, G. C., & Ide, S. (2007). Non-volcanic tremor and low-frequency earthquake swarms. *Nature*, *446*(7133), 305.

Silverii, F., D'Agostino, N., Métois, M., Fiorillo, F., & Ventafridda, G. (2016). Transient deformation of karst aquifers due to seasonal and multiyear groundwater variations observed by GPS in southern Apennines (Italy). *Journal of Geophysical Research: Solid Earth*, *121*, 8315–8337. https://doi.org/10.1002/2016JB013361

Socquet, A., Valdes, J. P., Jara, J., Cotton, F., Walpersdorf, A., Cotte, N., et al. (2017). An 8 month slow slip event triggers progressive nucleation of the 2014 Chile megathrust. *Geophysical Research Letters*, *44*, 4046–4053. https://doi.org/10.1002/2017GL073023

Sun, T., Wang, K., Linuma, T., Hino, R., He, J., Fujimoto, H., et al. (2015). Prevalence of viscoelastic relaxation after the 2011 Tohoku-Oki earthquake. *Nature*, *514*, 84–87. https://doi.org/10.1038/nature13778

Trubienko, O., Garaud, J.-D., & Fleitout, L. (2014). Models of postseismic deformation after megaearthquakes: The role of various rheological and geometrical parameters of the subduction zone. *Solid Earth Discussions*, *6*(1), 427–466. https://doi.org/10.5194/sed-6-427-2014

Valdés-Pineda, R., Canón, J., & Valdés, J. B. (2018). Multi-decadal 40- to 60-year cycles of precipitation variability in Chile (South America) and their relationship to the AMO and PDO signals. *Journal of Hydrology*, *556*, 1153–1170. https://doi.org/10.1016/j.jhydrol.2017.01.031

Vigny, C., Rudloff, A., Ruegg, J. C., Madariaga, R., Campos, J., & Alvarez, M. (2009). Upper plate deformation measured by GPS in the Coquimbo Gap, Chile. *Physics of the Earth and Planetary Interiors*, *175*(1), 86–95.

Vigny, C., Socquet, A., Peyrat, S., Ruegg, J.-C., Metois, M., Madariaga, R., et al. (2011). The 2010 Mw 8.8 Maule megathrust earthquake of central Chile, monitored by GPS. *Science*, *332*(6036), 1417–1421. https://doi.org/10.1126/science.1204132

Wahr, J., Khan, S. A., Dam, T., Liu, L., Angelen, J. H., Broeke, M. R., & Meertens, C. M. (2013). The use of GPS horizontals for loading studies, with applications to northern California and southeast Greenland. *Journal of Geophysical Research: Solid Earth*, *118*, 1795–1806. https://doi.org/10.1002/jgrb.50104

Wallace, L. M., & Beavan, J. (2010). Diverse slow slip behavior at the Hikurangi subduction margin, New Zealand. *Journal of Geophysical Research*, *115*, B12402. https://doi.org/10.1029/2010JB007717

Wallace, L. M., Kaneko, Y., Hreinsdóttir, S., Hamling, I., Peng, Z., Bartlow, N., et al. (2017). Large-scale dynamic triggering of shallow slow slip enhanced by overlying sedimentary wedge. *Nature Geoscience*, *10*(10), 765–770.

Wallace, L. M., Webb, S. C., Ito, Y., Mochizuki, K., Hino, R., Henrys, S., et al. (2016). Slow slip near the trench at the Hikurangi subduction zone, New Zealand. *Science*, *352*(6286), 701–704.

Wessel, P., Smith, W. H. F., Scharroo, R., Luis, J., & Wobbe, F. (2013). Generic Mapping Tools: Improved version released. *Eos, Transactions American Geophysical Union*, *94*(45), 409–410. https://doi.org/10.1002/2013EO450001

Willis, B. (1929). *Studies in comparative seismology: Earthquake conditions in Chile*. Washington: Carnegie Institution of Washington.

Wunsch, C., Heimbach, P., Ponte, R. M., Fukumori, I., & Members, E.-G. C. (2009). The global general circulation of the ocean estimated by the ECCO-consortium. *Oceanography*, *22*(2), 88–103.

Zigone, D., Rivet, D., Radiguet, M., Campillo, M., Voisin, C., Cotte, N., et al. (2012). Triggering of tremors and slow slip event in Guerrero, Mexico, by the 2010 Mw 8.8 Maule, Chile, earthquake. *Journal of Geophysical Research*, *117*, B09304. https://doi.org/10.1029/2012JB009160